

# The Effect of Nanoscale Nonuniformity of Oxygen Vacancy on Electrical and Reliability Characteristics of HfO<sub>2</sub> MOSFET Devices

Hokyung Park, Minseok Jo, Hyejung Choi, Musarrat Hasan, Rino Choi, Paul D. Kirsch, Chang Young Kang, Byoung Hun Lee, Tae-Wook Kim, Takhee Lee, and Hyunsang Hwang

**Abstract**—To understand the influence of oxygen vacancies in HfO<sub>2</sub> on the electrical and reliability characteristics, we have investigated area-dependent leakage-current characteristics of HfO<sub>2</sub> with large-area device and conducting atomic force microscopy (C-AFM). Unlike with the large-area analysis with typical capacitor and transistor, a clear evidence of oxygen vacancy was observed in nanoscale-area measurement using the C-AFM. Similar observations were made in various postdeposition annealing ambients to investigate the generation and reduction of oxygen vacancy in HfO<sub>2</sub>. With optimized postdeposition annealing for oxygen vacancy, significantly reduced charge trapping was observed in HfO<sub>2</sub> nMOSFET.

**Index Terms**—Charge trapping, conducting atomic force microscopy (C-AFM), hafnium oxide, oxygen vacancy.

## I. INTRODUCTION

HIGH- $\kappa$  GATE dielectrics have been investigated to replace silicon dioxide (SiO<sub>2</sub>) as the gate dielectric for future CMOS technologies [1]–[3]. Among the high- $\kappa$  dielectrics, the Hf-based dielectrics are intensively studied due to their compatibility with the conventional CMOS process [3]–[5]. However, to implement Hf-based dielectric into conventional CMOS process, threshold voltage ( $V_{th}$ ) instability and reliability degradation issues caused by charge trapping should be solved [6]–[8]. When physical thickness of high- $\kappa$  dielectric is decreased, a significant improvement of device performance was observed, owing to the reduction of charge-trap site [9]. But, without clear understanding on charge-trapping mechanism, a high-performance transistor with good reliability may not be achieved.

Recently, either by physical analysis or atomic simulation, oxygen vacancy was proposed to explain the origin of charge trapping in high- $\kappa$  dielectric [10]–[12]. Due to the analysis difficulty of nanoscale behavior with capacitor and transistor,

oxygen-vacancy generation and passivation during the fabrication process have not been clearly understood. For that reason, C-AFM was used to understand the nanoscale behavior of HfO<sub>2</sub> [13], [14]. However, a systematic nanoscale analysis of HfO<sub>2</sub> depending on postdeposition annealing (PDA) has not been carried out. In this letter, we will investigate the electrical characteristics of HfO<sub>2</sub> in nanosize area with C-AFM measurement and correlate this result with oxygen vacancy.

## II. EXPERIMENTS

After standard cleaning of 200-mm n-type silicon wafer, SiO<sub>x</sub> interfacial layer was formed with an ozone oxidizing method. A 3-nm-thick HfO<sub>2</sub> was deposited by atomic-layer-deposition method. Then, PDA was performed at 700 °C for 1 min in various ambients (NH<sub>3</sub>, N<sub>2</sub>, and O<sub>2</sub>). To observe the electrical characteristics depending on PDA, Pt/HfO<sub>2</sub> capacitor and TiN/HfO<sub>2</sub> MOSFET were fabricated by using the conventional CMOS process. To fabricate HfO<sub>2</sub> MOSFET with minimal interfacial layer regrowth and boron diffusion into a dielectric, one set of MOSFET samples was performed with PDA in NH<sub>3</sub> ambient. To understand the charge-trapping effect depending on the PDA, another set of MOSFET samples was performed with an additional O<sub>2</sub> PDA after the NH<sub>3</sub> PDA. Finally, forming gas annealing (H<sub>2</sub>/N<sub>2</sub> = 3%/97%) was performed at 400 °C for 30 min in atmospheric ambient.

For nanoscale-area analysis of HfO<sub>2</sub>, a C-AFM measurement in atmospheric ambient was employed. A Pt-coated Si cantilever was used as a nanosize tip. The size of the C-AFM tip is around 300 nm<sup>2</sup>. To measure the wide range of leakage current, a source and measure unit in Agilent 4155 was connected to the AFM system. To avoid the damage of the tip from ionic contamination during measurement, electrons were injected from the substrate [15].

## III. RESULTS AND DISCUSSION

Gate leakage-current density ( $J_g$ ) (at  $V_g - V_{fb} = 1$  V) and capacitance–voltage characteristics of 3-nm HfO<sub>2</sub> depending on PDA are shown in Fig. 1. Due to the uniform depositions of HfO<sub>2</sub> film, all measured spots showed uniform distribution of  $J_g$ . The reduction of  $J_g$  and the increase of equivalent oxide thickness (EOT) was observed in N<sub>2</sub> and O<sub>2</sub> PDA samples (around 0.2 nm) and can be explained by interfacial-layer regrowth during the PDA process.

Manuscript received September 18, 2007. This work was supported by the Center for Distributed Sensor Network, Gwangju Institute of Science and Technology, Gwangju, Korea. The review of this letter was arranged by Editor C.-P. Chang.

H. Park, M. Jo, H. Choi, M. Hasan, T.-W. Kim, T. Lee, and H. Hwang are with the Department of Materials Science and Engineering, Gwangju Institute of Science and Technology, Gwangju 500-712, Korea (e-mail: hwanghs@gist.ac.kr).

R. Choi is with the Inha University, Incheon 402-751, Korea.

P. D. Kirsch, C. Y. Kang, and B. H. Lee are with SEMATECH, Austin, TX 78741 USA.

Color versions of one or more of the figures in this letter are available online at <http://ieeexplore.ieee.org>.

Digital Object Identifier 10.1109/LED.2007.911992

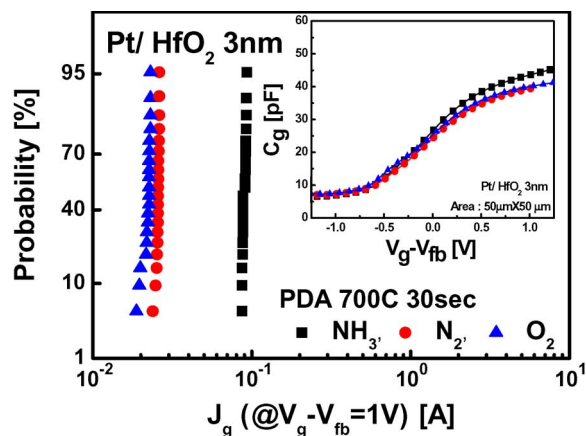


Fig. 1. Gate leakage-current density and capacitance–voltage characteristics of 3-nm HfO<sub>2</sub> depending on PDA. Gate leakage current of each sample was extracted at  $V_g - V_{fb} = 1$  V, and measured area is  $2.5 \times 10^{-5}$  cm<sup>2</sup>.

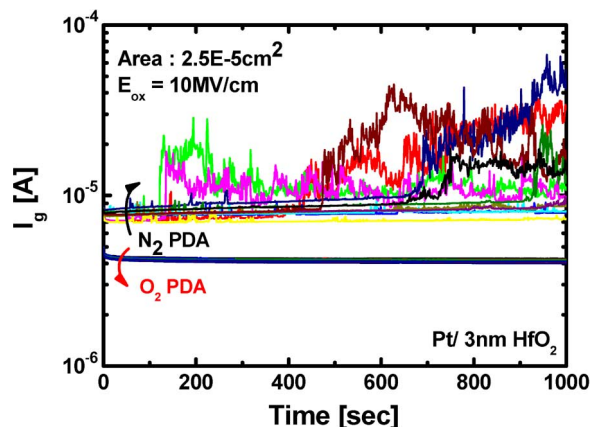


Fig. 2. Charge-trapping characteristics depending on N<sub>2</sub> and O<sub>2</sub> PDA. To maximize the charge trapping in HfO<sub>2</sub> layer, 10 MV/cm of electrical field ( $V_g - V_{fb}$ /EOT) stress was applied to the gate. At this field, electrons are injected through the triangular region of HfO<sub>2</sub> conduction band. To generalize the results, 12 different spots were measured for the same PDA condition.

To investigate the charge-trapping behavior depending on PDA, 10 MV/cm of constant field stress was applied to N<sub>2</sub> and O<sub>2</sub> PDA samples (Fig. 2). At this field, electrons are injected through the triangular region of HfO<sub>2</sub> conduction band, and charge trapping in HfO<sub>2</sub> layer can be maximized. The oxygen PDA sample showed a minimal charge trapping, whereas the sample with N<sub>2</sub> PDA showed a significant charge trapping and a soft breakdown during stress. Considering a similar accumulation capacitance after PDA, the increased charge trapping and soft breakdown in N<sub>2</sub> PDA might be explained by the increased charge-trap site in HfO<sub>2</sub>.

To clearly understand the dielectric property of HfO<sub>2</sub> depending on PDA, electrical characteristics in nanoscale regime were evaluated with C-AFM. Before nanoscale analysis of HfO<sub>2</sub>, 3-nm-thick SiO<sub>2</sub> was measured as a control (data not shown here). C-AFM measurement with SiO<sub>2</sub> showed a uniform current flow and breakdown field regardless of the measured spot and area, suggesting that the distribution of traps in SiO<sub>2</sub> is quite uniform. This uniform gate leakage current in SiO<sub>2</sub> also suggests that measurement error induced

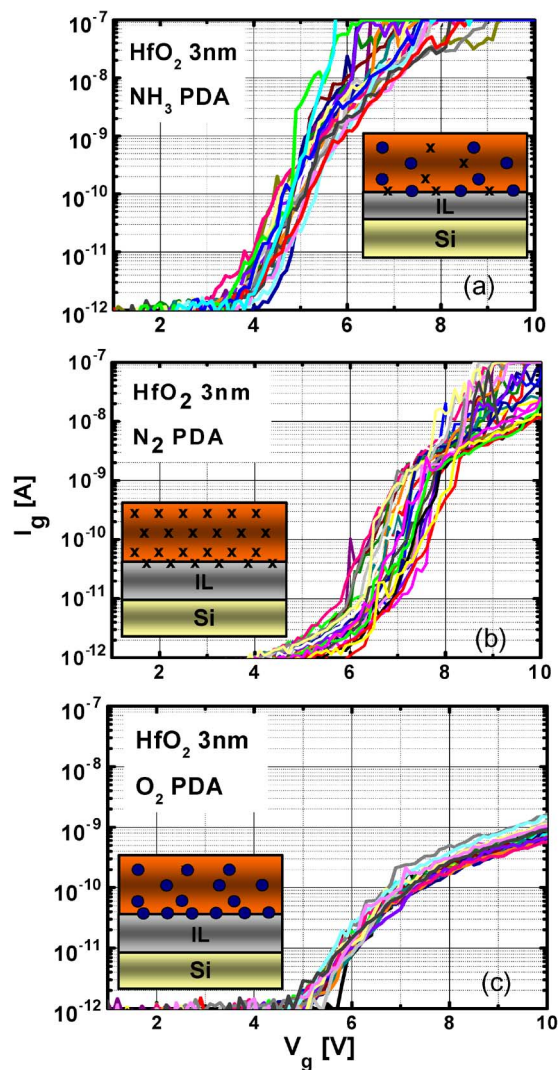


Fig. 3.  $I$ - $V$  characteristics of 3-nm HfO<sub>2</sub> in nanoscale area depending on PDA. PDA was performed at 700 °C for 1 min in (a) NH<sub>3</sub>, (b) N<sub>2</sub>, and (c) O<sub>2</sub> ambients. Inset represents the generation and passivation of oxygen vacancy depending on PDA.

by surface contamination is negligible. On the other hand, the current–voltage ( $I$ - $V$ ) characteristics of HfO<sub>2</sub> in nanoscale-area were somewhat different from that of SiO<sub>2</sub>. Fig. 3 shows the  $I$ - $V$  characteristics of HfO<sub>2</sub> depending on PDA. A wide distribution of gate leakage current ( $I_g$ ) was observed in HfO<sub>2</sub> with N<sub>2</sub> PDA. Compared with N<sub>2</sub> PDA, NH<sub>3</sub> PDA showed the reduction of  $I_g$  variation in low-voltage region (4–6 V). Considering the band bending of dielectric and the  $I$ - $V$  characteristics together, nitrogen incorporation is effective for the trap passivation in HfO<sub>2</sub> layer and reduces  $I_g$  variation. The weak improvement of  $I_g$  in high-voltage region ( $> 6$  V) can be understood by the reliability characteristics of thin SiO<sub>x</sub> interfacial layer [13]. However, even if nitrogen incorporation into HfO<sub>2</sub> helps the reduction of  $I_g$ , HfO<sub>2</sub> still showed the large variation of  $I_g$ . This result indicates that the origin of nanoscale nonuniformity of  $I_g$  in HfO<sub>2</sub> cannot be fully cured with nitrogen. Compared with NH<sub>3</sub> and N<sub>2</sub> PDA, the sample with O<sub>2</sub> PDA showed a significant reduction of  $I_g$  variation. Considering a similar EOT with N<sub>2</sub> PDA, the significant reduction of  $I_g$

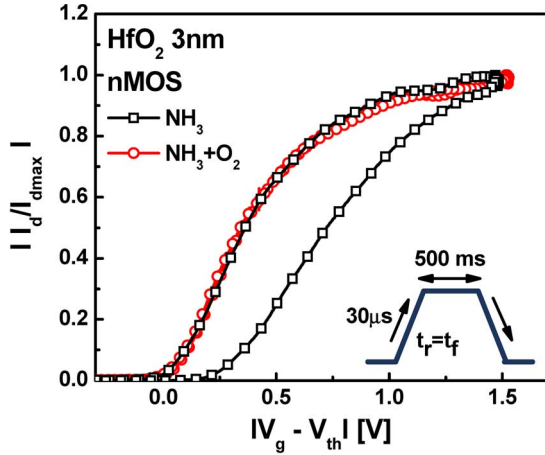


Fig. 4. Single pulsed  $I_d$ - $V_g$  characteristics of 3-nm  $\text{HfO}_2$  nMOSFET. Compared with  $\text{NH}_3$  PDA,  $\text{O}_2$  PDA followed by  $\text{NH}_3$  PDA showed a significant reduction of charge trapping during measurement.

variation after  $\text{O}_2$  PDA could not be explained with interfacial-layer regrowth. The reduction of  $I_g$  variation after  $\text{O}_2$  PDA can be explained by the successful passivation of oxygen-vacancy-related traps in  $\text{HfO}_2$  [10]. Based on these findings, the nanoscale nonuniformity of  $I_g$  in  $\text{HfO}_2$  should be explained by oxygen vacancy and can be cured with oxygen treatment.

The  $I_g$  variation in the nanoscale area can be understood with the inset of Fig. 3. During  $\text{NH}_3$  and  $\text{O}_2$  PDA, nitrogen and oxygen incorporated into  $\text{HfO}_2$  dielectric and passivated trap sites. However, during  $\text{N}_2$  PDA, only oxygen migration occurred due to the inert property of  $\text{N}_2$  gas. Thus, a wide variation of  $I_g$  was observed in  $\text{N}_2$  PDA because of the increased oxygen-vacancy site in the  $\text{HfO}_2$  layer.

The effects of oxygen-vacancy passivation on charge trapping and reliability were evaluated by single pulsed  $I_d$ - $V_g$  measurement (Fig. 4). Compared with  $\text{NH}_3$  PDA,  $\text{O}_2$  PDA followed by  $\text{NH}_3$  PDA showed a significant reduction of hysteresis. The significant reduction of hysteresis also suggests the effective passivation of oxygen vacancy in  $\text{HfO}_2$  layer.

#### IV. SUMMARY

The charge-trapping characteristics of the  $\text{HfO}_2$  and the effect of oxygen-vacancy site are clearly correlated with large and nanoscale-area analyses. C-AFM study of  $\text{HfO}_2$  in nanoscale-area showed that the nanoscale nonuniformity of gate leakage current is strongly dependent on the PDA conditions. The significant reduction of gate leakage-current nonuniformity after oxygen annealing indicates that the oxygen vacancy can be a major source of gate leakage current and origin of charge-trap sites in  $\text{HfO}_2$ . To achieve high-performance  $\text{HfO}_2$  transistor with good reliability, a careful optimization of dielectric properties to minimize oxygen vacancies is necessary.

#### REFERENCES

- [1] E. P. Gusev, A. Buchanan, E. Cartier, A. Kumar, D. DiMaria, S. Guha, A. Callegari, S. Zafar, P. C. Jamison, D. A. Neumayer, M. Copel, M. A. Gribelyuk, H. Okorn-Schmidt, C. D'Emic, P. Kozlowski, K. Chan, N. Bojarczuk, L.-A. Ragnarsson, P. Ronsheim, K. Rim, R. J. Fleming, A. Mocuta, and A. Ajmera, "Ultrathin high- $\kappa$  gate stacks for advanced CMOS devices," in *IEDM Tech. Dig.*, 2001, pp. 451–454.
- [2] J. C. Lee, H. J. Cho, C. S. Kang, S. Rhee, Y. H. Kim, R. Choi, C. Y. Kang, C. Choi, and M. Abkar, "High- $\kappa$  dielectrics and MOSFET characteristics," in *IEDM Tech. Dig.*, 2003, pp. 95–98.
- [3] T. Iwamoto, T. Ogura, M. Terai, H. Watanabe, H. Watanabe, N. Ikarashi, M. Miyamura, T. Tatsumi, M. Saitoh, A. Morioka, K. Watanabe, Y. Saito, Y. Yabe, T. Ikarashi, K. Masuzaki, Y. Mochizuki, and T. Mogami, "A highly manufacturable low power and high speed  $\text{HfSiO}$  CMOS FET with dual poly-Si gate electrodes," in *IEDM Tech. Dig.*, 2003, pp. 639–642.
- [4] S.-C. Song, Z. Zhang, C. Huffman, J. H. Sim, S. H. Bae, P. D. Kirsch, P. Majhi, R. Choi, N. Momen, and B. H. Lee, "Highly manufacturable advanced gate-stack technology for sub-45-nm self-aligned gate-first CMOSFETs," *IEEE Trans. Electron Device*, vol. 53, no. 5, pp. 979–989, May 2006.
- [5] H.-S. Jung, J.-H. Lee, S. K. Han, Y.-S. Kim, H. J. Lim, M. J. Kim, S. J. Doh, M. Y. Yu, N.-I. Lee, H.-L. Lee, T.-S. Jeon, H.-J. Cho, S. B. Kang, S. Y. Kim, I. S. Park, D. Kim, H. S. Baik, and Y. S. Chung, "A highly manufacturable MIPS (metal inserted poly-Si stack) technology with novel threshold voltage control," in *VLSI Symp. Tech. Dig.*, 2005, pp. 232–233.
- [6] B. H. Lee, C. D. Young, R. Choi, J. H. Sim, G. Bersuker, C. Y. Kang, R. Harris, G. A. Brown, K. Matthews, S. C. Song, N. Momen, J. Barnett, P. Lysaght, K. S. Choi, H. C. Wen, C. Huffman, H. Alshareef, P. Majhi, S. Gopalan, J. Peterson, P. Kirsh, H.-J. Li, J. Gutt, M. Gardner, H. R. Huff, P. Zeizoff, R. Murto, L. Larson, and C. Ramiller, "Intrinsic characteristics of fast transient charging effects (FCTE)," in *IEDM Tech. Dig.*, 2004, pp. 859–862.
- [7] S. Zafar, A. Kumar, E. Gusev, and E. Cartier, "Threshold voltage instabilities in high- $\kappa$  gate dielectric stacks," *IEEE Trans. Device Mater. Rel.*, vol. 5, no. 1, pp. 45–64, Mar. 2005.
- [8] H. Park, R. Choi, B. H. Lee, S.-C. Song, M. Chang, C. D. Young, G. Bersuker, J. C. Lee, and H. Hwang, "Decoupling of cold-carrier effects in hot-carrier reliability assessment of  $\text{HfO}_2$  gated nMOSFETs," *IEEE Electron Device Lett.*, vol. 27, no. 8, pp. 662–664, Aug. 2006.
- [9] P. D. Kirsch, S. C. Song, J. H. Sim, S. Krishnan, J. Gutt, J. Peterson, H.-J. Li, M. Quevedo-Lopez, C. D. Young, R. Choi, J. Barnett, N. Momen, K. S. Choi, C. Huffman, P. Majhi, M. Gardner, G. Brown, G. Bersuker, and B. H. Lee, "Mobility enhancement of ALD  $\text{HfO}_2/\text{TiN}$  gate stacks through improved charge trapping characteristics of 2.0 nm  $\text{HfO}_2$ ," in *Proc. ESSDERC*, 2005, pp. 367–370.
- [10] H. Takeuchi, D. Ha, and T.-J. King, "Observation of bulk  $\text{HfO}_2$  defects by spectroscopic ellipsometry," *J. Vac. Sci. Technol. A, Vac. Surf. Films*, vol. 22, no. 4, pp. 1337–1341, Jul. 2004.
- [11] K. Torii, H. Kitajima, T. Arikado, K. Shiraishi, S. Miyazaki, K. Yamabe, M. Boero, T. Chikyow, and K. Yamada, "Physical model of BTI, TDDB and SILC in  $\text{HfO}_2$ -based high- $\kappa$  gate dielectrics," in *IEDM Tech. Dig.*, 2004, pp. 859–862.
- [12] Y. P. Feng, A. T. L. Lim, and M. F. Li, "Negative- $U$  property of oxygen vacancy in cubic  $\text{HfO}_2$ ," *Appl. Phys. Lett.*, vol. 87, no. 6, p. 062 105, Aug. 2005.
- [13] L. Aguilera, M. Porti, M. Nafria, and X. Aymerich, "Charge trapping and degradation of  $\text{HfO}_2/\text{SiO}_2$  MOS gate stacks observed with enhanced CAFM," *IEEE Electron Device Lett.*, vol. 27, no. 3, pp. 157–159, Mar. 2006.
- [14] K. Kyuno, K. Kita, and A. Toriumi, "Evolution of leakage paths in  $\text{HfO}_2/\text{SiO}_2$  stacked gate dielectrics: A stable direct observation by ultrahigh vacuum conducting atomic force microscopy," *Appl. Phys. Lett.*, vol. 86, no. 6, p. 063 510, Feb. 2005.
- [15] M. Porti, M. Nafria, X. Aymerich, A. Olbrich, and B. Ebersberger, "Electrical characterization of stressed and broken down  $\text{SiO}_2$  films at a nanometer scale using a conductive atomic force microscope," *J. Appl. Phys.*, vol. 91, no. 4, pp. 2071–2079, Feb. 2002.